EUROPEAN ORGANIZATION FOR NUCLEAR RESEARCH

CERN-EP/2003-016
11 April 2003

Search for Stable and Long-Lived Massive Charged Particles in e^+e^- Collisions at $\sqrt{s} = 130 - 209$ GeV

The OPAL Collaboration

Abstract

A search for stable and long-lived massive particles of electric charge $|Q/e| = 1$ or fractional charges of 2/3, 4/3, and 5/3 is reported using data collected by the OPAL detector at LEP, at centre-of-mass energies from 130 to 209 GeV. These particles are assumed to be pair-produced in e^+e^- collisions and not to interact strongly. No evidence for the production of these particles was observed. Model-independent upper limits on the production cross-section between 0.005 and 0.028 pb have been derived for scalar and spin-1/2 particles with charge ± 1. Within the framework of the Constrained Minimal Supersymmetric Standard Model (CMSSM), this implies a lower limit of 98.0 (98.5) GeV on the mass of long-lived right (left)- handed scalar muons and scalar taus. Long-lived charged heavy leptons and charginos are excluded for masses below 102.0 GeV. For particles with fractional charge $\pm 2/3$, $\pm 4/3$ and $\pm 5/3$, the upper limit on the production cross-section varies between 0.005 and 0.020 pb. All mass and cross-section limits are derived at the 95% confidence level and are valid for particles with lifetimes longer than 10^{-6} s.

(To be submitted to Physics Letters B)

The OPAL Collaboration

G. Abbiendi[2], C. Ainsley[5], P.F. Åkesson[3], G. Alexander[22], J. Allison[16], P. Amaral[9], G. Anagnostou[1], K.J. Anderson[9], S. Arcelli[2], S. Asai[23], D. Axen[27], G. Azuelos[18,a], I. Bailey[26], E. Barberio[8,p], R.J. Barlow[16], R.J. Batley[5], P. Bechtle[25], T. Behnke[25], K.W. Bell[20], P.J. Bell[1], G. Bella[22], A. Bellerive[6], G. Benelli[4], S. Bethke[32], O. Biebel[31], O. Boeriu[10], P. Bock[11], M. Boutemeur[31], S. Braibant[8], L. Brigliadori[2], R.M. Brown[20], K. Buesser[25], H.J. Burckhart[8], S. Campana[4], R.K. Carnegie[6], B. Caron[28], A.A. Carter[13], J.R. Carter[5], C.Y. Chang[17], D.G. Charlton[1], A. Csilling[29], M. Cuffiani[2], S. Dado[21], A. De Roeck[8], E.A. De Wolf[8,s], K. Desch[25], B. Dienes[30], M. Donkers[6], J. Dubbert[31], E. Duchovni[24], G. Duckeck[31], I.P. Duerdoth[16], E. Etzion[22], F. Fabbri[2], L. Feld[10], P. Ferrari[8], F. Fiedler[31], I. Fleck[10], M. Ford[5], A. Frey[8], A. Fürtjes[8], P. Gagnon[12], J.W. Gary[4], G. Gaycken[25], C. Geich-Gimbel[3], G. Giacomelli[2], P. Giacomelli[2], M. Giunta[4], J. Goldberg[21], E. Gross[24], J. Grunhaus[22], M. Gruwé[8], P.O. Günther[3], A. Gupta[9], C. Hajdu[29], M. Hamann[25], G.G. Hanson[4], K. Harder[25], A. Harel[21], M. Harin-Dirac[4], M. Hauschild[8], C.M. Hawkes[1], R. Hawkings[8], R.J. Hemingway[6], C. Hensel[25], G. Herten[10], R.D. Heuer[25], J.C. Hill[5], K. Hoffman[9], D. Horváth[29,c], P. Igo-Kemenes[11], K. Ishii[23], H. Jeremie[18], P. Jovanovic[1], T.R. Junk[6], N. Kanaya[26], J. Kanzaki[23,u], G. Karapetian[18], D. Karlen[26], K. Kawagoe[23], T. Kawamoto[23], R.K. Keeler[26], R.G. Kellogg[17], B.W. Kennedy[20], D.H. Kim[19], K. Klein[11,t], A. Klier[24], S. Kluth[32], T. Kobayashi[23], M. Kobel[3], S. Komamiya[23], L. Kormos[26], T. Krämer[25], P. Krieger[6,l], J. von Krogh[11], K. Kruger[8], T. Kuhl[25], M. Kupper[24], G.D. Lafferty[16], H. Landsman[21], D. Lanske[14], J.G. Layter[4], A. Leins[31], D. Lellouch[24], J. Letts[o], L. Levinson[24], J. Lillich[10], S.L. Lloyd[13], F.K. Loebinger[16], J. Lu[27,w], J. Ludwig[10], A. Macpherson[28,i], W. Mader[3], S. Marcellini[2], A.J. Martin[13], G. Masetti[2], T. Mashimo[23], P. Mättig[m], W.J. McDonald[28], J. McKenna[27], T.J. McMahon[1], R.A. McPherson[26], F. Meijers[8], W. Menges[25], F.S. Merritt[9], H. Mes[6,a], A. Michelini[2], S. Mihara[23], G. Mikenberg[24], D.J. Miller[15], S. Moed[21], W. Mohr[10], T. Mori[23], A. Mutter[10], K. Nagai[13], I. Nakamura[23,V], H. Nanjo[23], H.A. Neal[33], R. Nisius[32], S.W. O'Neale[1], A. Oh[8], A. Okpara[11], M.J. Oreglia[9], S. Orito[23,*], C. Pahl[32], G. Pásztor[4,g], J.R. Pater[16], G.N. Patrick[20], J.E. Pilcher[9], J. Pinfold[28], D.E. Plane[8], B. Poli[2], J. Polok[8], O. Pooth[14], M. Przybycień[8,n], A. Quadt[3], K. Rabbertz[8,r], C. Rembser[8], P. Renkel[24], J.M. Roney[26], S. Rosati[3], Y. Rozen[21], K. Runge[10], K. Sachs[6], T. Saeki[23], E.K.G. Sarkisyan[8,j], A.D. Schaile[31], O. Schaile[31], P. Scharff-Hansen[8], J. Schieck[32], T. Schörner-Sadenius[8], M. Schröder[8], M. Schumacher[3], C. Schwick[8], W.G. Scott[20], R. Seuster[14,f], T.G. Shears[8,h], B.C. Shen[4], P. Sherwood[15], G. Siroli[2], A. Skuja[17], A.M. Smith[8], R. Sobie[26], S. Söldner-Rembold[16,d], F. Spano[9], A. Stahl[3], K. Stephens[16], D. Strom[19], R. Ströhmer[31], S. Tarem[21], M. Tasevsky[8], R.J. Taylor[15], R. Teuscher[9], M.A. Thomson[5], E. Torrence[19], D. Toya[23], P. Tran[4], I. Trigger[8], Z. Trócsányi[30,e], E. Tsur[22], M.F. Turner-Watson[1], I. Ueda[23], B. Ujvári[30,e], C.F. Vollmer[31], P. Vannerem[10], R. Vértesi[30], M. Verzocchi[17], H. Voss[8,q], J. Vossebeld[8,h], D. Waller[6], C.P. Ward[5], D.R. Ward[5], P.M. Watkins[1], A.T. Watson[1], N.K. Watson[1], P.S. Wells[8], T. Wengler[8], N. Wermes[3], D. Wetterling[11] G.W. Wilson[16,k], J.A. Wilson[1], G. Wolf[24], T.R. Wyatt[16], S. Yamashita[23], D. Zer-Zion[4], L. Zivkovic[24]

[1]School of Physics and Astronomy, University of Birmingham, Birmingham B15 2TT, UK
[2]Dipartimento di Fisica dell' Università di Bologna and INFN, I-40126 Bologna, Italy

[3]Physikalisches Institut, Universität Bonn, D-53115 Bonn, Germany
[4]Department of Physics, University of California, Riverside CA 92521, USA
[5]Cavendish Laboratory, Cambridge CB3 0HE, UK
[6]Ottawa-Carleton Institute for Physics, Department of Physics, Carleton University, Ottawa, Ontario K1S 5B6, Canada
[8]CERN, European Organisation for Nuclear Research, CH-1211 Geneva 23, Switzerland
[9]Enrico Fermi Institute and Department of Physics, University of Chicago, Chicago IL 60637, USA
[10]Fakultät für Physik, Albert-Ludwigs-Universität Freiburg, D-79104 Freiburg, Germany
[11]Physikalisches Institut, Universität Heidelberg, D-69120 Heidelberg, Germany
[12]Indiana University, Department of Physics, Bloomington IN 47405, USA
[13]Queen Mary and Westfield College, University of London, London E1 4NS, UK
[14]Technische Hochschule Aachen, III Physikalisches Institut, Sommerfeldstrasse 26-28, D-52056 Aachen, Germany
[15]University College London, London WC1E 6BT, UK
[16]Department of Physics, Schuster Laboratory, The University, Manchester M13 9PL, UK
[17]Department of Physics, University of Maryland, College Park, MD 20742, USA
[18]Laboratoire de Physique Nucléaire, Université de Montréal, Montréal, Québec H3C 3J7, Canada
[19]University of Oregon, Department of Physics, Eugene OR 97403, USA
[20]CLRC Rutherford Appleton Laboratory, Chilton, Didcot, Oxfordshire OX11 0QX, UK
[21]Department of Physics, Technion-Israel Institute of Technology, Haifa 32000, Israel
[22]Department of Physics and Astronomy, Tel Aviv University, Tel Aviv 69978, Israel
[23]International Centre for Elementary Particle Physics and Department of Physics, University of Tokyo, Tokyo 113-0033, and Kobe University, Kobe 657-8501, Japan
[24]Particle Physics Department, Weizmann Institute of Science, Rehovot 76100, Israel
[25]Universität Hamburg/DESY, Institut für Experimentalphysik, Notkestrasse 85, D-22607 Hamburg, Germany
[26]University of Victoria, Department of Physics, P O Box 3055, Victoria BC V8W 3P6, Canada
[27]University of British Columbia, Department of Physics, Vancouver BC V6T 1Z1, Canada
[28]University of Alberta, Department of Physics, Edmonton AB T6G 2J1, Canada
[29]Research Institute for Particle and Nuclear Physics, H-1525 Budapest, P O Box 49, Hungary
[30]Institute of Nuclear Research, H-4001 Debrecen, P O Box 51, Hungary
[31]Ludwig-Maximilians-Universität München, Sektion Physik, Am Coulombwall 1, D-85748 Garching, Germany
[32]Max-Planck-Institute für Physik, Föhringer Ring 6, D-80805 München, Germany
[33]Yale University, Department of Physics, New Haven, CT 06520, USA

[a] and at TRIUMF, Vancouver, Canada V6T 2A3
[c] and Institute of Nuclear Research, Debrecen, Hungary
[d] and Heisenberg Fellow
[e] and Department of Experimental Physics, Lajos Kossuth University, Debrecen, Hungary
[f] and MPI München
[g] and Research Institute for Particle and Nuclear Physics, Budapest, Hungary
[h] now at University of Liverpool, Dept of Physics, Liverpool L69 3BX, U.K.
[i] and CERN, EP Div, 1211 Geneva 23
[j] and Manchester University

[k] now at University of Kansas, Dept of Physics and Astronomy, Lawrence, KS 66045, U.S.A.
[l] now at University of Toronto, Dept of Physics, Toronto, Canada
[m] current address Bergische Universität, Wuppertal, Germany
[n] now at University of Mining and Metallurgy, Cracow, Poland
[o] now at University of California, San Diego, U.S.A.
[p] now at Physics Dept Southern Methodist University, Dallas, TX 75275, U.S.A.
[q] now at IPHE Université de Lausanne, CH-1015 Lausanne, Switzerland
[r] now at IEKP Universität Karlsruhe, Germany
[s] now at Universitaire Instelling Antwerpen, Physics Department, B-2610 Antwerpen, Belgium
[t] now at RWTH Aachen, Germany
[u] and High Energy Accelerator Research Organisation (KEK), Tsukuba, Ibaraki, Japan
[v] now at University of Pennsylvania, Philadelphia, Pennsylvania, USA
[w] now at TRIUMF, Vancouver, Canada
[*] Deceased

1 Introduction

Many searches for massive new particles predicted by extensions to the Standard Model (SM) assume that these particles decay promptly at the primary interaction vertex. Such searches are not sensitive to long-lived heavy particles which do not decay within the detectors. There exist, however, a number of models which predict such long-lived particles. For example, in the Constrained Minimal Supersymmetric Standard Model (CMSSM), for certain choices of the parameters, sleptons or charginos could be long-lived [1]. R-parity violating supersymmetric (SUSY) models [2] also allow for long-lived heavy particles and a fourth-generation heavy lepton could be stable [3]. In gauge-mediated supersymmetry, if the SUSY-breaking energy scale is sufficiently high [4], sleptons could be long-lived. Some models beyond the SM also predict the existence of particles with fractional electric charge. Previous searches for long-lived massive charged particles have been performed by the LEP collaborations with data taken at the Z^0 resonance [5], as well as with data taken at higher centre-of-mass energies, up to 209 GeV [6, 7].

This paper describes an update to a search for long-lived particles, referred to here as $\mathrm{X}^{\pm}$, with $m_{\mathrm{X}} > m_{\mathrm{Z}}/2$, and charge $|Q/e| = 1$ or $2/3$, pair-produced in the reaction $\mathrm{e}^+\mathrm{e}^- \to \mathrm{X}^+\mathrm{X}^-$. This search has been described in detail in [6]. In this paper we also search for particles with fractional charges $4/3$ and $5/3$. All fractionally-charged particles are assumed to be colourless and non-strongly-interacting. To make the search for these particles as model independent as possible, only minimal calorimetric information has been used. Due to their large mass these particles would have anomalously high or low ionization energy loss $\mathrm{d}E/\mathrm{d}x$ in the tracking chambers. This search is therefore primarily based on the precise $\mathrm{d}E/\mathrm{d}x$ measurement provided by the OPAL jet chamber. The data were collected by the OPAL detector during 1995-2000, at centre-of-mass energies from 130 GeV to 209 GeV corresponding to a total integrated luminosity of 693.1 pb^{-1} as reported in Table 1.

2 The OPAL Detector

A complete description of the OPAL detector can be found in Ref. [8]. Here only a brief overview is given. The central detector comprised a system of tracking chambers, providing track reconstruction over 96% of the full solid angle[1] inside a 0.435 T uniform magnetic field parallel to the beam axis. It consisted of a two-layer silicon microstrip vertex detector, a high-precision vertex drift chamber (CV) with axial and stereo wires, a large-volume jet chamber and a set of z-chambers measuring the track coordinates along the beam direction.

The jet chamber (CJ) is the most important detector for this analysis. It was divided into 24 azimuthal sectors, each equipped with 159 sense wires. Up to 159 position and $\mathrm{d}E/\mathrm{d}x$ measurements per track were thus possible, with a precision of $\sigma_{r\phi} \approx 135\,\mu$m and $\sigma_z \approx 6$ cm. When a track was matched with z-chamber hits and hits on the stereo wires of the vertex chamber (CV), the uncertainty on its z coordinate was ≈ 1 mm. The tracking detectors, located inside the magnet coil, provided a track momentum measurement with a resolution of $\sigma_p/p \approx \sqrt{(0.02)^2 + (0.0015 \cdot p_t)^2}$ for tracks with the full number of hits (p_t, in GeV, is the momentum transverse to the beam direction) and a resolution on the ionization energy loss

[1] The OPAL right-handed coordinate system is defined such that the z-axis is in the direction of the electron beam, the x-axis points towards the centre of the LEP ring, and θ and ϕ are the polar and azimuthal angles, defined relative to the $+z$- and $+x$-axes, respectively. The radial coordinate is denoted by r.

measurement of approximately 2.8% for $\mu^+\mu^-$ events with a large number of usable hits for $\mathrm{d}E/\mathrm{d}x$ measurement [9].

A lead-glass electromagnetic calorimeter (ECAL) located outside the magnet coil covered the full azimuthal range with good hermeticity in the polar angle range of $|\cos\theta| < 0.984$. The magnet return yoke was instrumented for hadron calorimetry covering the region $|\cos\theta| < 0.99$ and was surrounded by four layers of muon chambers. Electromagnetic calorimeters close to the beam axis completed the geometrical acceptance down to 24 mrad on both sides of the interaction point.

The ionization energy loss $\mathrm{d}E/\mathrm{d}x$ produced by a charged particle is a function of the electric charge Q and of $\beta\gamma = p/m$, where p is the momentum and m the mass of the particle [9]. Figure 1 shows the distribution of $\mathrm{d}E/\mathrm{d}x$ as a function of the apparent momentum, p/Q. Standard particles of charge ±1 (e, μ, π, p, K) with high momentum ($p > 0.1\sqrt{s}$) have $\mathrm{d}E/\mathrm{d}x$ between 9 and 11 keV/cm. Massive particles with charge ±1 are expected to yield $\mathrm{d}E/\mathrm{d}x > 11$ keV/cm for high-mass values, $m_{\mathrm{X}} > 0.36\sqrt{s}$, or $\mathrm{d}E/\mathrm{d}x < 9$ keV/cm for low-mass values, $m_{\mathrm{X}} < 0.27\sqrt{s}$. The $\mathrm{d}E/\mathrm{d}x$ measurement therefore provides a good tool for particle identification in these high- and low-mass regions. Massive particles with charge $\pm2/3$ would have $\mathrm{d}E/\mathrm{d}x > 11$ keV/cm for high mass values, $m_{\mathrm{X}} > 0.45\sqrt{s}$ or $\mathrm{d}E/\mathrm{d}x < 9$ keV/cm for low-mass values, $m_{\mathrm{X}} < 0.35\sqrt{s}$. The expected $\mathrm{d}E/\mathrm{d}x$ for massive particles of charge $\pm4/3$ and $\pm5/3$ is greater than 11 keV/cm for all mass ranges. The search for massive particles with charge $\pm1/3$ was not possible because the typical $\mathrm{d}E/\mathrm{d}x$ deposit of these particles would be too close to the instrumental noise level.

3 Monte Carlo Simulation

Several different Monte Carlo programs were used to generate the signal process $\mathrm{e^+e^-} \to \mathrm{X^+X^-}$. Signal events of the type $\mathrm{e^+e^-} \to \tilde{\ell}^+\tilde{\ell}^-$ ($\tilde{\ell}^\pm$ being a charged scalar lepton) were generated at several centre-of-mass energies up to 206 GeV using SUSYGEN [10]. The generated charged scalar leptons are not allowed to decay, therefore simulating a signal from heavy charged stable scalar particles. Similarly, events of the type $\mathrm{e^+e^-} \to \mathrm{L^+L^-}$ and $\mathrm{e^+e^-} \to \mathrm{Q\bar{Q}}$, where $\mathrm{L}^\pm$ are stable heavy spin-1/2 leptons, and Q, $\bar{\mathrm{Q}}$ are colourless stable heavy spin-1/2 particles with charge 2/3, 4/3, and 5/3, were generated at the same energies, using the EXOTIC [11] generator. All signal samples were generated with 1000 events per mass point with mass m_{X} ranging from 45 GeV to the kinematic limit for the centre-of-mass energy considered. The mass points were generated every 5 GeV with a finer binning of 1 GeV in the mass regions where we expect lower selection efficiencies. For the purpose of detector simulation and particle interactions, all particles were treated as heavy muons. The simulation of $\mathrm{d}E/\mathrm{d}x$ in the central jet chamber of OPAL accounted for the charge, mass and momentum of the particle, as described above.

The background was estimated using simulations of all Standard Model processes (two-fermion, four-fermion and two-photon processes) for all centre-of-mass energies from 130 to 206 GeV. Small differences in the centre-of-mass energies of data and background Monte Carlo samples have a negligible effect on the analysis.

The contribution to the background from two-fermion final states was estimated using BHWIDE [12] for the $\mathrm{e^+e^-}$ final states and KORALZ [13] and KK2f [14] for the $\mu^+\mu^-$ and $\tau^+\tau^-$ states. Hadronic two-fermion events, $\mathrm{q\bar{q}}$, were simulated using PYTHIA [15]. For the two-photon background, the PYTHIA [15], PHOJET [16] and HERWIG [17] Monte Carlo genera-

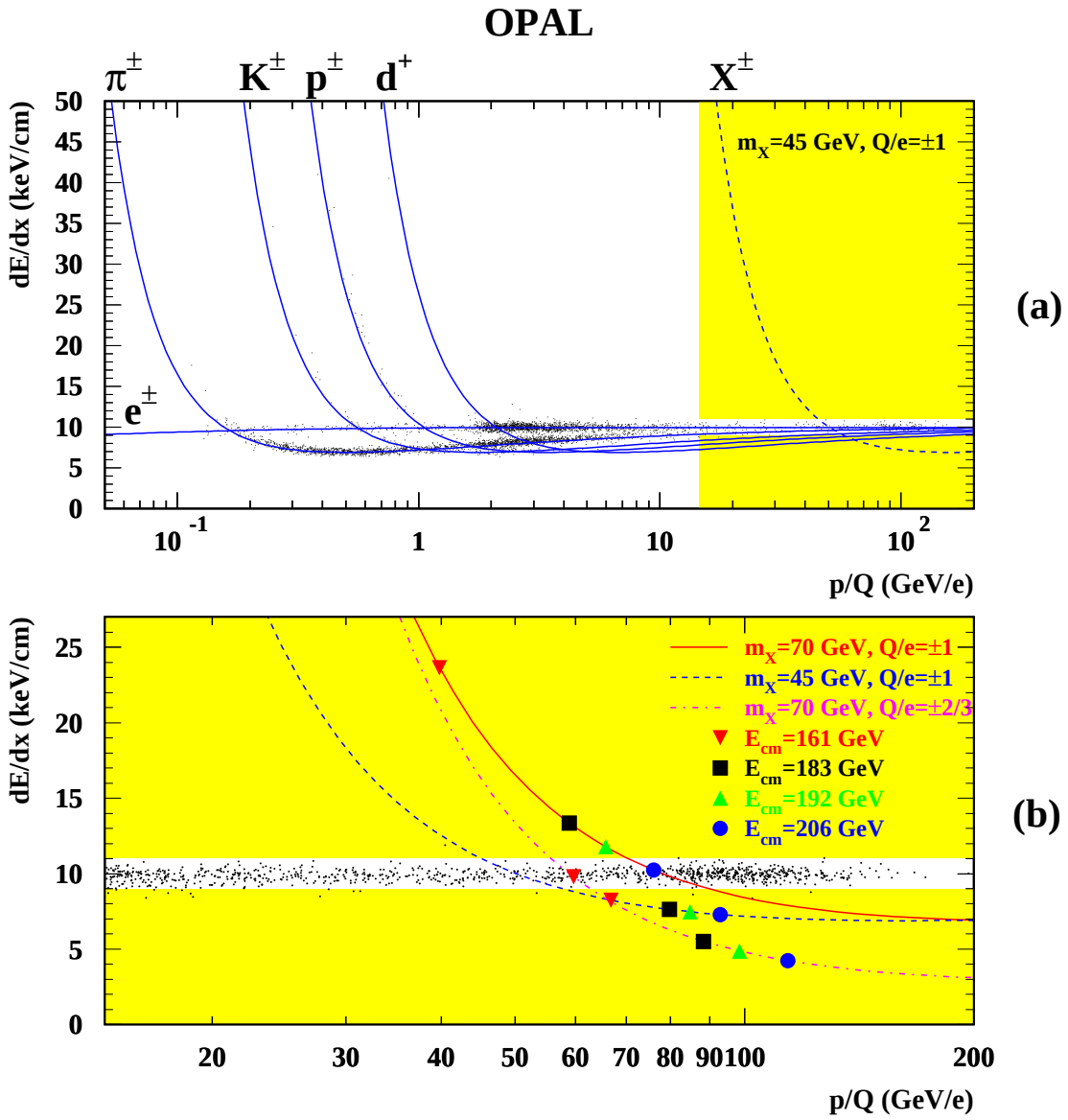

Figure 1: *(a) The distribution of the ionization energy loss,* $\mathrm{d}E/\mathrm{d}x$*, of tracks in the CJ detector, as a function of the apparent momentum,* p/Q*, for a sample of the data collected in the year 2000. The two shaded regions are the search regions. The momentum lower limit of the search regions is defined by the preselection cut* $p > 0.07\sqrt{s}$*. No cut has been applied to the data, apart from a cutoff of* $p_t > 0.1$ *GeV made to reject low momentum tracks trapped in the jet chamber volume.*
(b) Expanded view of the search regions. The theoretical curves for heavy long-lived particles are shown with example points from various centre-of-mass energies. In $\mathrm{e^+e^-} \to \mathrm{X^+X^-}$ *events, the momentum of the* $\mathrm{X}^{\pm}$ *particles of a given mass is fixed by* $\sqrt{s}$*.*

tors were used for $e^+e^-q\bar{q}$ final states and the Vermaseren [18] and the BDK [19] generators for all $e^+e^-\ell^+\ell^-$ final states. Four-fermion final states were simulated with grc4f [20], which takes into account interference between all diagrams. All generated signal and background events were processed through the full simulation of the OPAL detector [21]; the same event analysis chain was applied to the simulated events and to the data.

4 Data Analysis

Pair-produced stable or long-lived massive charged particles would manifest themselves in events with two back-to-back tracks. Assuming they would not interact strongly, these particles would not produce hadronic showers. Since they are massive, they would not produce electromagnetic showers either. For these reasons, the considered events would be very similar to $\mu^+\mu^-$ events, the only difference being the higher mass of the particles, which yields a different $\mathrm{d}E/\mathrm{d}x$ for the same momentum.

A preselection similar to the one described in [6] is used for the analyses. Several criteria have been loosened in order to increase the sensitivity to high-mass particles. The criteria are listed below:

P1 Events are rejected if the total multiplicity of tracks in the central detector and clusters in the ECAL is greater than 26. Cosmic ray events are rejected as in [22]. Bhabha events are identified by requiring two energetic and collinear clusters in the electromagnetic calorimeter, these events are then rejected.

P2 Events are required to contain at least two tracks in the central detector, each satisfying basic quality criteria[2] and having a momentum $p > 0.07\sqrt{s}$, a momentum transverse to the beam axis $p_t > 0.025\sqrt{s}$, a polar angle satisfying $|\cos\theta| < 0.97$ and at least 20 CJ hits usable for $\mathrm{d}E/\mathrm{d}x$ measurement. The two selected tracks are required to have opposite electric charge.

P3 To reduce background from two-photon events, the total visible energy[3] of the event is required to be $E_{\mathrm{vis}} > 0.14\sqrt{s}$ and the acoplanarity angle[4] between the two tracks is required to be $\phi_{\mathrm{acop}} < 20^\circ$.

P4 Events containing an isolated ECAL cluster with an energy greater than 5 GeV are rejected to reduce background from events with initial state radiation. Isolation is defined as an angular separation of more than 15° from the closest track.

P5 It is required that $\frac{E_1}{p_1} + \frac{E_2}{p_2} < 0.2$, where $p_{1,2}$ are the momenta of the two selected tracks and $E_{1,2}$ denote the energies of the ECAL clusters associated to the tracks. This further reduces the contribution from Bhabha scattering events. No other tracks with $p > 0.5$ GeV and no unassociated clusters with $E > 3$ GeV should be found in a cone of

[2]The distance between the beam axis and the track at the point of closest approach (PCA) must be less than 1 cm; the z-coordinate of the PCA must be less than 40 cm; the innermost hit of the track measured by the jet chamber must be closer than 75 cm to the beam axis.

[3]The visible energy, the visible mass and the total transverse momentum of the event are calculated using tracks and calorimeter clusters, correcting for double counting as described in [24].

[4]The acoplanarity angle, ϕ_{acop}, is defined as 180° minus the angle between the two tracks in the $r-\phi$ plane.

10° half-opening angle around each of the two selected tracks. Criterion P5 is not used in the fractionally-charged particles analysis since their interaction properties with the calorimeters are unknown. This reduces the dependence on calorimeter response around the candidate tracks.

After the preselection, the background is dominated by $e^+e^- \to \mu^+\mu^-$ events, with a small contribution from $e^+e^- \to \tau^+\tau^-$ and two-photon $e^+e^-\mu^+\mu^-$ events. The effect of the preselection cuts on the all data samples and various Monte Carlo background processes, for the search for $|Q/e| = 1$ particles, is shown in Table 2.

Nominal $\sqrt{s}(GeV)$ bins	$\mathcal{L}$ (pb^{-1})	$\|Q/e\| = 1$ search		Fractional charge search	
		candidates	background	candidates	background
133	10.7	0	0.02±0.16	0	0.24±0.19
161	10.0	0	0.11±0.11	0	0.20±0.32
172	10.4	0	0.001±0.04	0	0.08±0.10
183	56.3	0	0.13±0.33	1	0.37±0.95
189	172.3	0	0.17±0.28	1	0.90±1.41
192	29.0	0	0.03±0.35	0	0.10±0.42
196	72.5	0	0.14±0.40	0	0.22±0.47
200	74.0	0	0.08±0.33	0	0.14±0.43
202	37.0	0	0.00±0.18	0	0.07±0.19
205	87.4	0	0.17±0.43	0	0.34±0.76
207	133.5	0	0.26±0.66	1	0.52±1.16
Total	693.1	0	1.1±1.3	3	3.2±2.4

Table 1: *The number of candidate events and the expected background at all energies, for the search for $|Q/e| = 1$ and fractionally-charged particles. The errors quoted include both statistical and systematic effects. In the second column, the integrated luminosity is given for each energy. The data collected in the year 2000 were delivered at various centre-of-mass energies, up to $\sqrt{s} = 209$ GeV. For this analysis they have been separated in two bins, the first one, referred to as 205 GeV, with $\sqrt{s} < 206$ GeV and an average $\sqrt{s}$ of 204.7 GeV, and the second one, referred to as 207 GeV, with $\sqrt{s} \geq 206$ GeV and an average $\sqrt{s}$ of 206.6 GeV.*

4.1 Search for particles with unit charge

The search strategy has been simplified with respect to [6] and now relies entirely on $\mathrm{d}E/\mathrm{d}x$ information. A sample $\mathrm{d}E/\mathrm{d}x$ distribution for data and simulated Monte Carlo events is shown in Figure 2. The kinematic selection is no longer used. This new strategy has been applied to all data samples. The preselected events are retained if they satisfy the following requirements on $\mathrm{d}E/\mathrm{d}x$:

A1 Both high-momentum tracks must have either $\mathrm{d}E/\mathrm{d}x > 11$ keV/cm or $\mathrm{d}E/\mathrm{d}x < 9$ keV/cm.

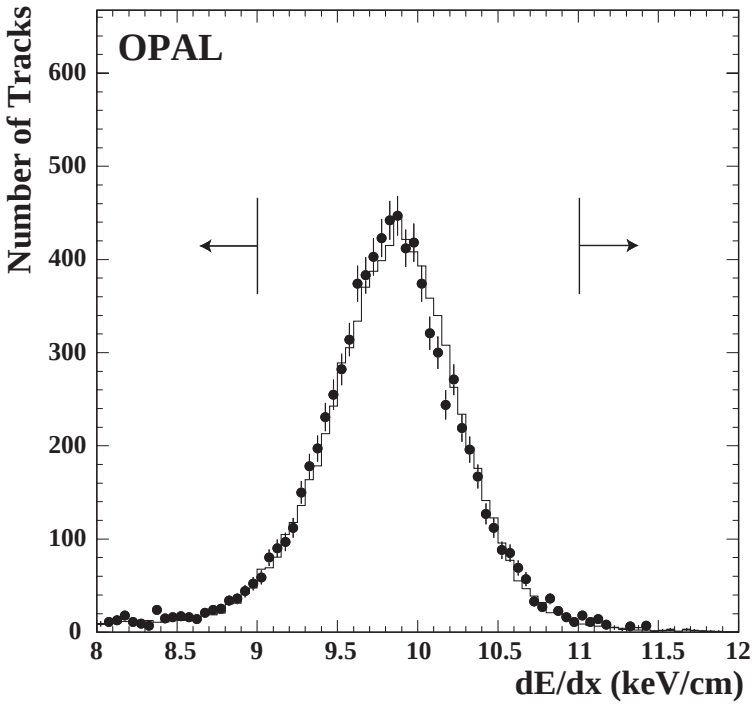

Figure 2: dE/dx *distribution for data and Monte Carlo simulation at* $\sqrt{s} = 189$ *GeV after the preselection cut* **P4**. *The arrows show the accepted region.*

A2 The probability that the dE/dx measurements for either track were consistent with one of the standard particles (e, μ, π, p, K) must be less than 30%. This removes background from poorly measured SM particles.

Cuts	Data	Background Simulation						Signal MC (%)		
		Total	e^+e^-	$\mu^+\mu^-$	$\tau^+\tau^-$	$e^+e^-\ell^+\ell^-$	Others	ϵ_{45}	ϵ_{55}	ϵ_{80}
P1–2	20199	19572.0	9292.8	4015.2	1305.4	3428.9	1529.7	96.6	97.5	97.2
P3–4	15935	15447.4	7439.8	3327.2	1081.0	2952.8	646.6	92.5	93.0	94.3
P5	4995	4956.6	<1.0	3098.7	76.5	1671.3	110.1	92.3	92.3	94.3
A1,A2	0	1.1	<1.0	0.01	0.01	1.1	0.03	85.7	73.4	94.3

Table 2: *For the* $|Q/e| = 1$ *analysis, the numbers of events remaining after each cut for all data collected at the various centre-of-mass energies and for various Monte Carlo background processes normalised to the integrated luminosity of the data ("*Others*" refers to* $e^+e^- \to q\bar{q}$ *and* e^+e^- *→ four-fermion processes). When no candidate events are selected in the Monte Carlo, a 68% CL upper limit on the number of events is used as the statistical uncertainty. In the last three columns, the efficiencies for* $\tilde{\ell}^+\tilde{\ell}^-$ *are given (in percent) for* $m_X = 45, 55, 80$ *GeV at* $\sqrt{s} = 207$ *GeV.*

The effect of cuts **A1-A2** for all data and simulated events can be seen in Table 2. No candidate event is found. The expected backgrounds at the various centre-of-mass energies are shown in Table 1. The total background, summed over all energies, is estimated to be 1.1±1.3 events, where the uncertainty quoted includes both statistical and systematic effects.

The detection efficiency for spin-0 particles varies between 75 and 90% for masses $m_X < 0.27\sqrt{s}$ or $m_X > 0.36\sqrt{s}$. The efficiency drops significantly in the region $0.27\sqrt{s} < m_X <$

$0.36\sqrt{s}$, but as data sets collected at different centre-of-mass energies ($\sqrt{s}$) are combined, a reasonable selection efficiency is achieved for all mass values up to close to the kinematic limit. The selection efficiencies of all Monte Carlo samples at all $\sqrt{s}$ are parametrised as a function of $\beta\gamma = p/m_{\mathrm{X}} = \sqrt{s/4m_X^2 - 1}$ of the particle. This parametrisation is used to calculate the efficiency for all masses at each centre-of-mass energy, using linear interpolation. For spin-1/2 particles, the efficiencies are 2-9% lower than for spin-0 particles due to the different angular distribution of the tracks. We analyse each centre-of-mass energy separately, then combine the results for the final cross-section limits.

4.2 Search for particles with fractional charges

To search for particles with fractional charges of 2/3, 4/3, and 5/3 the selection criteria **P1** through **P4**, followed by **A1** and **A2** are used. The results after each cut for all data samples and various Monte Carlo background processes are shown in Table 3. For charge 2/3 the selection efficiency is between 75 and 90% for most of the mass range, while for charges 4/3 and 5/3 the efficiency is above 90% for the whole mass range. After this selection, one candidate survives in the data sample at $\sqrt{s} = 183$ GeV, one at $\sqrt{s} = 189$ GeV, and one at $\sqrt{s} = 207$ GeV, while no candidate is left in any of the other data sets. The masses of the candidates are reconstructed for charge 2/3 using the $\mathrm{d}E/\mathrm{d}x$ and momentum information, while for charge 4/3 and 5/3 kinematic information only is used. The reconstructed masses, track momenta and $\mathrm{d}E/\mathrm{d}x$ values of the candidate events are reported in Table 4. The selected events and the expected background at each centre-of-mass energy are shown in Table 1. The total background, summed over all energies, is estimated to be 3.2±2.4 events, where the uncertainty quoted includes both statistical and systematic effects.

Cuts	Data	Background Simulation						Signal MC (%)		
		Total	$\mathrm{e^+e^-}$	$\mu^+\mu^-$	$\tau^+\tau^-$	$\mathrm{e^+e^-}\ell^+\ell^-$	Others	2/3	4/3	5/3
P1–2	20199	19572.0	9292.8	4015.2	1305.4	3428.9	1529.7	93.1	97.6	97.8
P3–4	15935	15447.4	7439.8	3327.2	1081.0	2952.8	646.6	89.7	94.8	94.7
A1,A2	3	3.2	0.7	0.03	0.5	1.4	0.5	86.3	94.8	94.7

Table 3: *For fractional charges analyses, the numbers of events remaining after each cut for all data collected at the various centre-of-mass energies and for various Monte Carlo background processes normalised to the integrated luminosity of the data ("*Others*" refers to* $\mathrm{e^+e^-} \to \mathrm{q\bar{q}}$ *and* $\mathrm{e^+e^-} \to$ *four-fermion processes). In the last three columns, the efficiencies are given (in percent) for* $|Q/e| = 2/3, 4/3, 5/3$ *at* $m_{\mathrm{X}} = 70$ *GeV and* $\sqrt{s} = 207$ *GeV.*

4.3 Systematic uncertainties

The main sources of systematic uncertainties for this analysis are discussed below and reported in Table 5, for both the signal efficiency and the background estimate:

- The errors on the Monte Carlo modeling of ϕ_{acop}, E_{vis} and $\mathrm{d}E/\mathrm{d}x$ are estimated by comparing the distributions of these variables for data and background Monte Carlo. The relative difference between the averages of the distributions is used to increase or

$\sqrt{s}$ (GeV)	p_1 (GeV)	p_2 (GeV)	$(\mathrm{d}E/\mathrm{d}x)_1$ (keV/cm)	$(\mathrm{d}E/\mathrm{d}x)_2$ (keV/cm)	Masses (GeV)		
					$\lvert Q/e\rvert = \frac{2}{3}$	$\lvert Q/e\rvert = \frac{4}{3}$	$\lvert Q/e\rvert = \frac{5}{3}$
183	64 ± 15	19 ± 30	11.04 ± 0.62	20.48 ± 1.00	49.6 ± 11.9	95.9 ± 9.4	-
189	30 ± 2	29 ± 15	11.17 ± 0.39	19.85 ± 0.95	24.9 ± 1.3	85.9 ± 1.0	80.7 ± 1.6
207	77 ± 8	71 ± 8	11.06 ± 0.34	11.13 ± 0.36	61.7 ± 4.7	-	-

Table 4: *Information on the candidate events selected by the fractionally-charged analysis. The momentum and* $\mathrm{d}E/\mathrm{d}x$ *of each track is reported together with the reconstructed masses for the* $|Q/e| = 2/3, 4/3, 5/3$ *hypothesis. The candidate mass is not reported when the reconstruction procedure gives a kinematically inconsistent result.*

Quantity	Systematic uncertainty (%)		
	Signal		Background
	High efficiency region	Low efficiency region	
ϕ_{acop}	0.0-1.2		0.0
E_{vis}	0.0-2.1		0.0
$\mathrm{d}E/\mathrm{d}x$	0.0-0.3	0.0-27	<0.008
MC statistics	0.6-2.6	0.8-21	58-157
Interpolation	0.0-2.7	0.0-35	-
MC generator	-		5.9-300
Double tracks	-		2.9
Luminosity	0.22-0.68		
Total	0.7-3.6	1.3-39	90-309

Table 5: *Relative systematic uncertainties in the signal efficiency associated with the various quantities used for the* $|Q/e| = 1$ *search. The ranges given cover all centre-of-mass energies. The systematic errors vary slightly with centre-of-mass energy, but strongly with* m_{X} *for the signal. For this reason the two regions are reported: high efficiency (*$m_{\mathrm{X}}/\sqrt{s} < 0.27$ *or* $m_{\mathrm{X}}/\sqrt{s} > 0.36$*) and low efficiency (*$0.27 < m_{\mathrm{X}}/\sqrt{s} < 0.36$*).*

decrease the value of the cut on the relevant variable in order to decrease the overall signal efficiency and background estimate. The difference between the reduced efficiency and the one obtained with the nominal selection is taken as the systematic uncertainty due to the modeling of the variable under consideration. This estimate of the error is more conservative than the one obtained by smearing the $\mathrm{d}E/\mathrm{d}x$ values of the tracks.

- The MC statistical uncertainty, due to the limited number of signal events generated, has been computed using a binomial formula. For background processes the large relative statistical uncertainty is due to the limited number of background events selected.

- The uncertainty due to the linear interpolation of the signal detection efficiency is estimated as the difference between the interpolated values and the efficiency obtained at mass points where MC signal samples were generated, when that mass point was omitted from the interpolation procedure.

- For background processes of the type $\mathrm{e^+e^-}\ell^+\ell^-$, the Vermaseren [18] generator has been used as the reference generator. The difference in the background expectation obtained by using BDK [19] instead of Vermaseren has been considered as the uncertainty on the MC generator.

- Two tracks separated by a distance smaller than 2.5 mm could be unresolved and reconstructed as a single track with a high $\mathrm{d}E/\mathrm{d}x$ value. Events with unresolved double tracks are potential backgrounds for this search. The systematic uncertainty introduced by the modeling of the double track resolution in the Monte Carlo samples has been estimated to be 2.9 percent.

The absolute uncertainty on the background is reported by centre-of-mass energy in Table 1. The uncertainty introduced on the integrated luminosity [25] is also reported in Table 5. At a given centre-of-mass energy the different systematic uncertainties are assumed to be independent, so that the total systematic uncertainty is calculated as the quadratic sum of the individual uncertainties. The Monte Carlo modeling of $\mathrm{d}E/\mathrm{d}x$, the Vermaseren-BDK generator, and luminosity uncertainties are assumed to be correlated between centre-of-mass energies, while the other systematic uncertainties are assumed to be independent.

5 Results

The numbers of candidates found in the search for particles with charge $|Q/e|$=1 and fractional charges are summarised for all energies in Table 1, together with the expected backgrounds. The data show no significant excess above the expected background from Standard Model processes.

Model-independent cross-section upper limits have been computed for the pair-production of massive charged long-lived particles, combining the results from all centre-of-mass energies, assuming s-channel production. The cross-section dependence on the energy is taken to be β^3/s for spin-0 particles and $\frac{\beta}{s}(1-\frac{\beta^2}{3})$ for spin-1/2 particles, where $\beta = p/E \simeq \sqrt{1-4m_{\mathrm{X}}^2/s}$. In evaluating upper limits, the candidates are counted in mass intervals centred on their central mass values and $\pm 2\sigma$ wide (where σ is the error on the mass estimate of the candidates as reported in Table 4). In the case in which the mass could not be reconstructed the candidates were considered in the whole mass range (from 45 GeV to the kinematic limit for that event). A likelihood-ratio method [26] was used to determine an upper limit for the cross-section. The total systematic error is incorporated into the limits following the prescription of Ref. [27].

In Figure 3(a), the 95% C.L. upper limit on the cross-section at $\sqrt{s} = 206.6$ GeV is shown for spin-0 particles of charge $\pm$ 1. The 95% C.L. upper limit on the pair-production cross-section varies from 0.005 to 0.028 pb in the mass range $45 < m_{\mathrm{X}} < 101$ GeV. The bump in the mass range of $52 < m_{\mathrm{X}} < 70$ GeV is due to the low efficiencies described in section 4.1. The cross-section limits are compared with the predicted cross-sections [10] for pair-production of right- and left-handed smuons and staus to determine mass limits. For these two slepton species, the production cross-section does not depend on the CMSSM parameters but only on the slepton mass. The 95% C.L. lower mass limits are 98.0 GeV and 98.5 GeV for the mass of right- and left-handed smuons and staus, respectively, as shown in Figure 3(a).

Figure 3(b) shows the 95% C.L. upper limit on the cross-section at $\sqrt{s} = 206.6$ GeV for spin-1/2 particles of charge $\pm$1. The limit varies from 0.005 to 0.024 pb in the mass range $45 < m_{\mathrm{X}} < 100$ GeV. This limit must be compared with the predicted cross-sections for chargino production [10] and heavy charged lepton production [11, 28]. For the chargino limits, the CMSSM parameters have been chosen to minimise the predicted chargino cross-section at every chargino mass value (assuming a heavy sneutrino, $m_{\tilde{\nu}} > 500$ GeV), without any

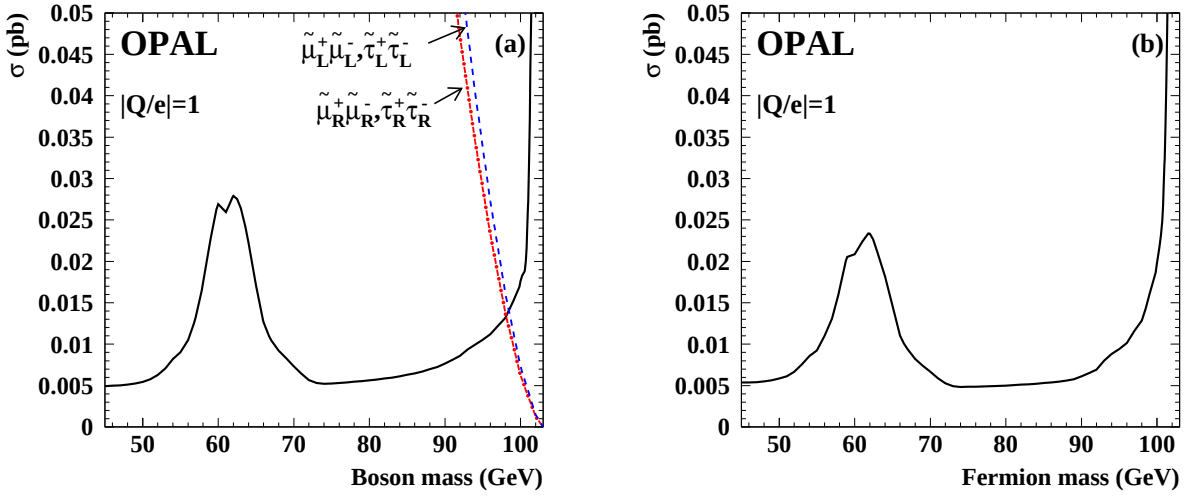

Figure 3: *Model-independent 95% C.L. upper limits on the pair-production cross-section of spin-0 (a) and spin-1/2 (b) heavy long-lived non-strongly-interacting particles of charge ±1 as a function of their mass (solid line) at* $\sqrt{s} = 206.6$ *GeV. The bump observed between masses of 52 and 70 GeV is due to the drop in efficiency where the* $\mathrm{d}E/\mathrm{d}x$ *expected for signal crosses the band of* $\mathrm{d}E/\mathrm{d}x$ *values expected for standard particles. The CMSSM predicted cross-sections for right-handed (dash-dotted line) and left-handed (dashed line) smuons and staus are also shown in (a). The 95% C.L. lower limits on the masses of these sleptons are at the crossing point between the experimental limit and theoretical prediction.*

restriction on the mass of the lightest neutralino. A 95% C.L. lower limit on the masses of long-lived charginos, of 102.0 GeV, is obtained for every choice of the CMSSM parameters. The 95% C.L. lower limit on the heavy charged lepton mass is also 102.0 GeV.

Figure 4(a) shows the 95% C.L. upper limit on the cross-section at $\sqrt{s} = 206.6$ GeV for spin-1/2 particles of charge ±2/3. The limit varies between 0.005 and 0.020 pb in the mass range $45 < m_{\mathrm{X}} < 101$ GeV. Figures 4(b) and 4(c) show the 95% C.L. upper limit on the cross-section at $\sqrt{s} = 206.6$ GeV for spin-1/2 particles of charge ±4/3 and of charge ±5/3, respectively. For spin-0 particles with fractional charge the cross-section upper limits are slightly higher than for spin-1/2 particles. This is due to the difference in angular distributions.

All results obtained are valid for non-strongly-interacting colourless particles with a lifetime longer than 10^{-6} s. This lifetime restriction is obtained by considering the heaviest (and therefore slowest) particles excluded by this search, and then requiring that the decay probability of these particles at a flight distance larger than 3.0 m be greater than 95%. For lower mass values the results are also valid for shorter lifetimes.

6 Summary and Conclusions

A search was performed for pair-production of stable and long-lived massive particles not subject to strong interactions, with charge $|Q/e| = 1$ or fractional charges of 2/3, 4/3, and 5/3. The

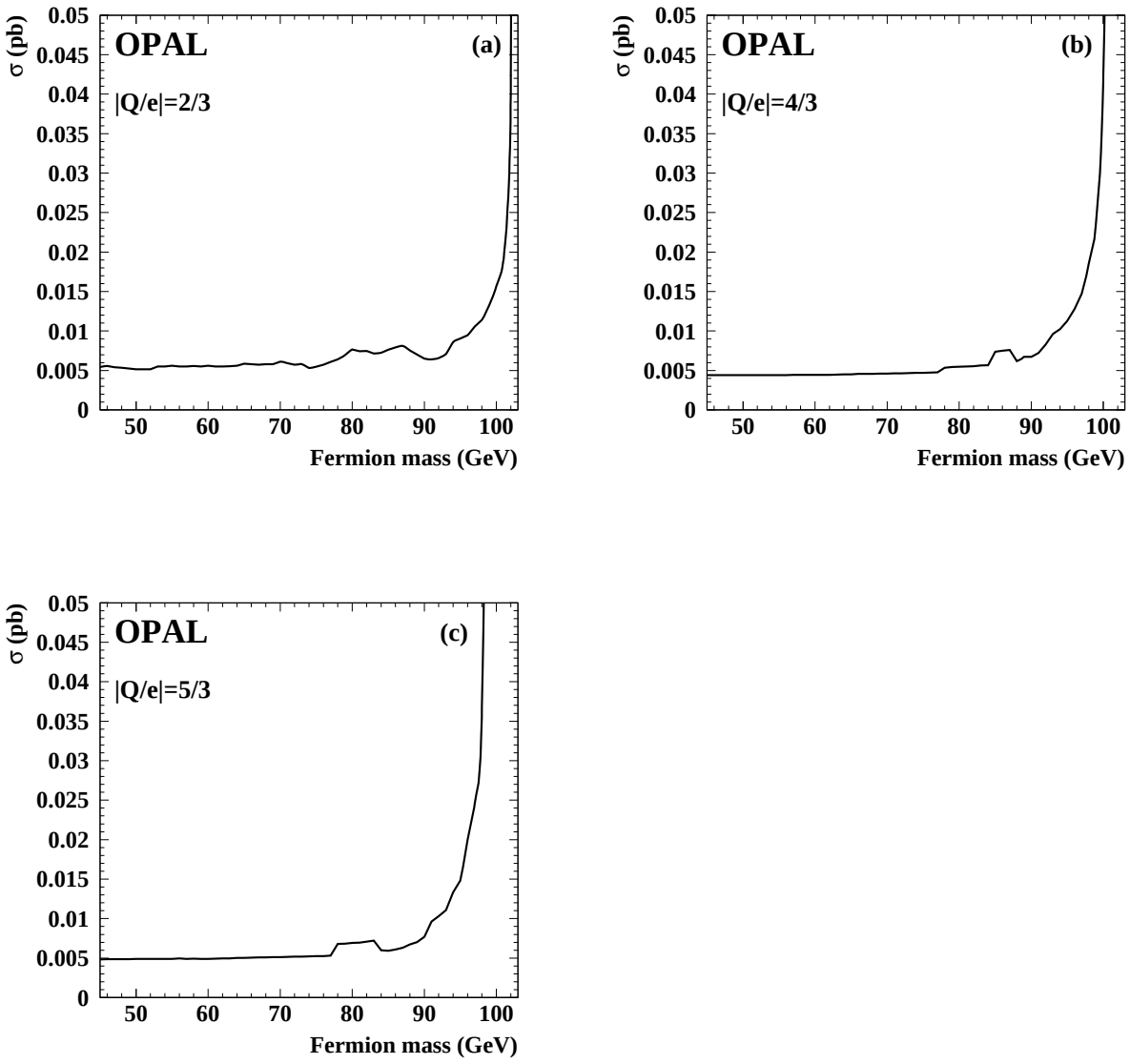

Figure 4: *Model-independent 95% C.L. upper limits on the pair-production cross-section as a function of mass of spin-1/2 heavy long-lived non-strongly-interacting particles of charge (a) $|Q/e| = \pm 2/3$, (b) $|Q/e| = \pm 4/3$ and (c) $|Q/e| = \pm 5/3$, at $\sqrt{s} =$ 206.6 GeV.*

primary tool used in this search was the precise $\mathrm{d}E/\mathrm{d}x$ measurement provided by the OPAL jet chamber. No evidence for the production of such particles was observed. For s-channel production, the upper limits on the cross-section vary between 0.005 and 0.026 pb in the mass range explored for particles of charge ± 1. Within the framework of the CMSSM, lower mass limits have been obtained: 98.0 GeV for right-handed and 98.5 GeV for the left-handed smuons and staus. Charged long-lived massive leptons and long-lived charginos with masses smaller than 102.0 GeV are excluded. For particles with fractional charge $\pm 2/3$, $\pm 4/3$ and $\pm 5/3$, the upper limits on the production cross-section vary between 0.005 and 0.020 pb in the range $45 < m_{\mathrm{X}} < 95$ GeV. The above limits are valid at the 95% C.L. for particles with lifetimes

longer than 10^{-6} s.

Acknowledgements

We particularly wish to thank the SL Division for the efficient operation of the LEP accelerator at all energies and for their close cooperation with our experimental group. In addition to the support staff at our own institutions we are pleased to acknowledge the
Department of Energy, USA,
National Science Foundation, USA,
Particle Physics and Astronomy Research Council, UK,
Natural Sciences and Engineering Research Council, Canada,
Israel Science Foundation, administered by the Israel Academy of Science and Humanities,
Benoziyo Center for High Energy Physics,
Japanese Ministry of Education, Culture, Sports, Science and Technology (MEXT) and a grant under the MEXT International Science Research Program,
Japanese Society for the Promotion of Science (JSPS),
German Israeli Bi-national Science Foundation (GIF),
Bundesministerium für Bildung und Forschung, Germany,
National Research Council of Canada,
Hungarian Foundation for Scientific Research, OTKA T-038240, and T-042864,
The NWO/NATO Fund for Scientific Reasearch, the Netherlands.

References

[1] H. P. Nilles, Phys. Rep. **110** (1984) 1;
H. E. Haber and G. L. Kane, Phys. Rep. **117** (1985) 75.

[2] H. Dreiner, *"An Introduction to Explicit R-parity Violation"*, Perspective on Supersymmetry, ed. G.L Kane, **462**, and hep-ph/9707435.

[3] E. Nardi, E. Roulet and D. Tommasini, Phys. Lett. **B344** (1995) 225.

[4] S. Dimopoulos, S. Thomas and J. D. Wells, Nucl. Phys. **B488** (1997) 39;
S. Ambrosanio, G. D. Kribs and S. P. Martin, Phys. Rev. **D56** (1997) 1761;
G. F. Giudice and R. Rattazzi, Phys. Rep. **322** (1999) 419.

[5] ALEPH Collab., D. Decamp *et al.*, Phys. Lett. **B303** (1993) 198;
DELPHI Collab., P. Abreu *et al.*, Phys. Lett. **B247** (1990) 157;
OPAL Collab., K. Ahmet *et al.*, Phys. Lett. **B252** (1990) 290;
OPAL Collab., R. Akers *et al.*, Z. Phys. **C67** (1995) 203.

[6] OPAL Collab., R. Ackerstaff *et al.*, Phys. Lett. **B433** (1998) 195.

[7] ALEPH Collab., R. Barate *et al.*, Phys. Lett. **B405** (1997) 379;
DELPHI Collab., P. Abreu *et al.*, Phys. Lett. **B478** (2000) 65;

DELPHI Collab., P. Abreu *et al.*, Phys. Lett. **B503** (2001) 34;
L3 Collab., P. Achard *et al.*, Phys. Lett. **B517** (2001) 75.

[8] OPAL Collab., K. Ahmet *et al.*, Nucl. Instr. Meth. **A305** (1991) 275;
P. P. Allport *et al.*, Nucl. Instr. Meth. **A324** (1993) 34;
P. P. Allport *et al.*, Nucl. Instr. Meth. **A346** (1994) 476;
S. Anderson *et al.*, Nucl. Instr. Meth. **A403** (1998) 326.

[9] M. Hauschild *et al.*, Nucl. Instr. Meth. **A314** (1992) 74;
M. Hauschild, Nucl. Instr. Meth. **A379** (1996) 436.

[10] S. Katsanevas and S. Melachroinos, in *"Physics at LEP2"*, ed. G. Altarelli, T. Sjöstrand and F. Zwirner, CERN 96-01, vol. 2, (1996) 328;
S. Katsanevas and P. Morzwitz, Comp. Phys. Comm. **112** (1998) 227.

[11] R. Tafirout and G. Azuelos, Comp. Phys. Comm. **126** (2000) 244.

[12] S. Jadach *et al.*, in *"Physics at LEP2"*, eds. G. Altarelli, T. Sjöstrand and F. Zwirner, CERN 96–01, vol.2, (1996) 229;
S. Jadach, W. Placzek and B.F.L. Ward, Phys. Lett. **B390** (1997) 298.

[13] S. Jadach, B.F.L. Ward and Z. Wąs, Comp. Phys. Comm. **79** (1994) 503.

[14] S. Jadach, B.F.L. Ward and Z. Wąs, Comp. Phys. Comm. **130** (2000) 260.

[15] T. Sjöstrand and M. Bengtsson, Comp. Phys. Comm. **43** (1987) 367;
"PYTHIA 5.7 and JETSET 7.4, Physics and Manual", CERN-TH. 7112/93 (revised August 1995);
T. Sjöstrand, Comp. Phys. Comm. **82** (1994) 74;
T. Sjöstrand, Comp. Phys. Comm. **135** (2001) 238.

[16] R. Engel and J. Ranft, Phys. Rev. **D54** (1996) 4244;
R. Engel, Z. Phys. **C66** (1995) 203.

[17] G. Marchesini *et al.*, Comp. Phys. Comm. **67** (1992) 465.

[18] R. Bhattacharya, J. Smith and G. Grammer, Phys. Rev. **D15** (1977) 3267;
J. Smith, J.A.M. Vermaseren and G. Grammer, Phys. Rev. **D15** (1977) 3280;
J. Smith, J.A.M. Vermaseren and G. Grammer, Phys. Rev. **D19** (1979) 137.

[19] F.A.Berends, P.H. Daverveldt and R. Kleiss, Nucl. Phys. **B253** (1985) 421;
F.A.Berends, P.H. Daverveldt and R. Kleiss, Comp. Phys. Comm. **40** (1986) 271;
F.A.Berends, P.H. Daverveldt and R. Kleiss, Comp. Phys. Comm. **40** (1986) 285;
F.A.Berends, P.H. Daverveldt and R. Kleiss, Comp. Phys. Comm. **40** (1986) 309.

[20] J. Fujimoto *et al.*, Comp. Phys. Comm. **100** (1997) 128.

[21] J. Allison *et al.*, Nucl. Instr. Meth. **A317** (1992) 47.

[22] OPAL Collab., R. Akers *et al.*, Z. Phys. **C61** (1994) 19.

[23] S. Robins, *"A Study of Bhabha Scattering at LEP"*, Ph.D. Thesis (1991), Queen Mary, U. of London, RALT-136.

[24] OPAL Collab., M.Z. Akrawy *et al.*, Phys. Lett. **B253** (1991) 511.

[25] OPAL Collab., K. Ackerstaff *et al.*, Phys. Lett. **B391** (1997) 221.

[26] A. G. Frodesen, O. Skeggestad and T. Tofte, *"Probability and Statistics in Particle Physics"*, Universitetsforlaget, 1979, ISBN 82-00-01-01906-3;
S. L. Meyer, *"Data Analysis for Scientists and Engineers"*, John Wiley and Sons, 1975, ISBN 0-471-59995-6.

[27] R. D. Cousins and V. L. Highland, Nucl. Instr. Meth. **A320** (1992) 331.

[28] A. Djouadi, Z. Phys. **C63** (1994) 317.